Using an industrial braiding machine to upscale the production and modulate the design of electrospun medical yarns

R.E. Abhari[a,*], P.A. Mouthuy[a], A. Vernet[b], J.E. Schneider[b], C.P. Brown[a], A.J. Carr[a]

[a] Nuffield Department of Orthopaedics, Rheumatology and Musculoskeletal Sciences, University of Oxford, Old Road, Oxford OX37LD, UK
[b] Wellcome Trust Centre for Human Genetics, Division of Cardiovascular Medicine, Radcliffe Department of Medicine, University of Oxford, Oxford, UK

ARTICLE INFO

ABSTRACT

While electrospun multifilaments have shown initial promise as medical yarns, their development has been restricted to short sections of hand-braided yarns. Integrating electrospun material into existing industrial braiding production lines would enable the modulation of yarn properties and an increased production rate to meet the demand for clinical trials. In this study, we used an industrial braiding machine to manufacture multifilament polydioxanone yarns with various filament numbers and carrier arrangements. The resulting yarns were characterized by mercury porosimetry, mechanical and pull through testing and compared to clinically used braided Vicryl and monofilament polydioxanone (PDS) sutures. Electrospun yarns were significantly more porous (67%) compared with Vicryl (28%) and PDS sutures (0%), and possessed the classic toe region reminiscent of native tissue. Pull through testing revealed that the structural configuration of electrospun yarns allowed for more energy dissipation. These findings suggest that upscaling the production of braided yarns is critical for designing medical yarns with required properties for clinical applications.

1. Introduction

Textile manufacturing is widely used in the medical market today to create dressings and medical yarns, such as sutures. Medical yarns are mostly produced by braiding, which offers some advantages over other textile methods, such as reduced fraying of the yarn, slight improvement in mechanical strength, and better control over structural properties such as porosity and pore size [1]. To date, braided medical yarns are predominantly manufactured from inert fibres, which are melt extruded from synthetic polymers, and their development is largely driven by industry. However, the recent academic interest in regenerative medicine is driving research towards 'bioactive' medical yarns that both mechanically approximate tissue, like current sutures, but also harness biophysical cues to drive cell directed repair.

For torn tissues with a poor intrinsic healing capacity, it is suggested that bioactive medical yarns made by electrospinning could be used during primary repair to better guide tissue regeneration. Electrospinning, a process by which nano- and microscale fibres are drawn out from a polymer solution using electrical charges, has received recent attention in the field of regenerative medicine [2]. Electrospun fibres mimic the extracellular matrix of soft tissues, as well as have a high surface area to volume ratio and a high porosity to promote cellular infiltration. Although densely aligned electrospun fibres

collected as sheets are biologically more advantageous than randomly organized fibres [3], they present significant mechanical, structural, and production limitations, which has prevented the implementation of as-spun materials in biomedical applications, such as sutures, stents, or drug delivery devices. The production of continuous bundles of fibres, known as filaments, opens the possibility of creating multifilament braided yarns with a hierarchical structure more similar to that of native tissue [1,4–11].

Braiding electrospun filaments into multifilament yarns has shown initial promise for soft tissue applications. Braided yarns have been shown to support tenogenic differentiation of human mesenchymal stem cells (hMSCs) and displayed similar mechanical behavior to native tendons [6,8,9]. To date, braided electrospun yarns have only been manufactured by hand into short sections, which limits the control over structural properties, the reproducibility of the product, and the overall production volume [1,5,6,8,9,12]. The delay in upscaling hand-made yarns to an industrial machine can be partially attributed to the sensitivity of the electrospinning process and the difficulty in producing continuous filaments, thereby hindering the further processing of these filaments for use with conventional textile machinery. Moreover, electrospun fibres are delicate and sensitive to mechanical damage and environmental degradation, meaning that some textile machinery is currently not suitable for scaling up electrospinning technology.

Together these challenges have limited the commercialization and clinical translation of many promising electrospun products in development.

We have recently developed a technique to produce sufficiently long and robust filaments, opening up the possibility of exploring braiding with an industrial machine [13,14]. Shifting the production of electrospun yarns to an industrial machine would lead to a higher degree of control over the yarn's structural properties than can be achieved with hand-braided yarns, as well as a wider variety of braiding designs to be explored by adjusting the orientation and distribution of fibres. Moreover, the use of an industrial machine can increase rate of production to meet the demand for clinical trials and later commercialisation [15]. Despite the potential of semi-automating the production of braided electrospun yarns, the use of an industrial machine has not been explored yet.

The objective of this study was two-fold: (1) to investigate the feasibility of using an industrial braiding machine with electrospun filaments, and (2) to design and manufacture yarns with various structural and mechanical properties. We hypothesized that it would be feasible to use an industrial braiding machine to modulate the properties and increase the rate of production of multifilament yarns. To demonstrate these hypotheses, electrospun polydioxanone filaments were braided using a Variation Braiding Machine into multifilament yarns with various filament numbers and carrier arrangements. The resulting yarns were characterized in terms of their porosity, mechanical behavior, and pull through properties.

2. Materials and methods

2.1. Electrospun monofilaments

Polymer solutions were made by dissolving polydioxanone (PDO, Sigma-Aldrich; viscosity 1.5–2.2 dL/g; T_g −10 to −5 °C; T_m 110–115 °C) in HFIP solvent (Apollo Scientific; 1,1,1,3,3,3, -hexafluora-2-propanol) at a 7% weight to volume ratio with a compound that changes the conductivity of the solvent, and stirred for 24 h before electrospinning. PDO is an attractive biodegradable polymer for use as a biomaterial, as it has a good safety profile with mild foreign body reaction and complete degradation between 5 months to one year, depending on manufacturing and processing conditions [13,16,17]. HFIP was chosen for its easy dissolution in the polymer and its fast evaporation in electrospinning conditions [18]. Measuring residual HFIP solvent is something that we intend to investigate more in the near future, however previous *in vitro* and *in vivo* work have shown no adverse effect and this has also been confirmed in other studies using this solvent [7,11].A custom electrospinning apparatus with a single nozzle and a stainless steel wire collector was used to fabricate continuous electrospun filaments [13]. A sketch of the electrospinning setup is given in the supplementary material as Supplementary Fig. 1. The solution feed rate was 0.8 mL/h, wire feed rate was 0.5 mm/s and the filaments spun under an electric field of 7.2 kV. The filaments were detached from the collecting wire and then manually stretched until resistance was felt (around 3.5 times their length), to increase the length and align the submicron fibres in the direction of the thread [13]. The average diameter of the electrospun fibres in the drawn filaments was 1.03 ± 0.3 μm and they were kept at room temperature of 25 °C in a desiccator until used for braiding.

2.2. Braided suture manufacturing

Braided multifilament sutures were made using a Variation Braiding Machine (VF 1/(4–32)-140, Herzog Braiding Machine, Oldenburg, Germany), an industrial braiding machine with manually changeable crossings, enabling the production of braids using 4 to 32 carriers. Four different braids composed of 12, 16, 20, and 24 filaments were made using 12, 8, 20, and 24 fine yarn carriers (carrier type AFDh 80, Herzog,

Oldenburg, Germany), respectively. The number of filaments for each braid was chosen based on the projected braid size falling in the desired yarn diameter range of 0.5–1 mm, a size range suitable for suture use. Following braiding assembly, the yarns were thermally annealed at 65 °C for 3 h, following previous work [14]. An optical micrometer (Keyence LS-7010MR laser with Keyence LS-7601 monitor, Milton Keynes, UK) was used to measure suture diameter by averaging 5 measurements, which was then converted to United States Pharmacopeia (USP) suture sizing standardisation. Finally, a Plugable Optical Digital Microscope (Plugable USB2-micro-250X, Redmond, WA, USA) was used to obtain images of the final yarns.

2.3. Scanning electron microscopy (SEM)

Scanning electron microscopy (Evo LS15 Variable Pressure Scanning Electron Microscope, Carl Zeiss AG, Germany) images from each braided sample were taken. The samples were washed with phosphate buffered saline (PBS, Sigma-Aldrich, St. Louis, MO, USA), cut, and coated with gold using a SC7620 Mini Sputter Coater System (Quorum Technologies Ltd, Laughton, UK) prior to mounting on the SEM machine. Samples were analysed in high vacuum mode to examine macroscopic morphology, surface texture, and braid angle of braided electrospun sutures. Images were captured at 50X and 150X magnifications and fibre diameter was determined using ImageJ software (National Institute of Health, Bethesda, MD, USA).

2.4. MicroCT analysis

Braided yarns were scanned over a length of 1 mm using micro-computed tomography (μCT). The yarns were placed in a tube that was mounted vertically on the μCT scanner (SkyScan 1172, SkyScan, Kontich, Belgium). The samples were scanned at an isotropic pixel size of 1.58μm. The scan parameters were set at a voltage of 40 kV; a current of 250 mA without filter and 900 projections were used. The images were reconstructed using NRecon software (SkyScan 1172, SkyScan, Kontich, Belgium) using the Feldkamp algorithm with a beam-hardening correction of 40% and a smoothing of 4. The reconstructed images were analysed using ImageJ software (National Institute of Health, Bethesda, MD, USA) in order to measure the yarn's surface area, diameter, and overall porosity.

2.5. Mercury porosimetry

Porosity and pore size distribution was determined by mercury intrusion technique using an Autopore IV 9500 mercury porosimeter (Micromeritics Instrument Co, Norcross, GA, USA). The porosimeter had a max pressure range of 33,000 psia and a measurable pore size range of 360 μm to 0.005 μm. Electrospun sutures were cut into sections weighing 70 mg and placed in the cup of the penetrometer (s/n = 14, 3 bulb, 0.412 stem, powder). The penetrometer was first passed through both the low-pressure port where the gases are evacuated from the penetrometer and then backfilled with mercury, and then through the high-pressure port. Samples were run with a mercury filing pressure of 0.49 psia and an equilibration time of 10 s. Two experimental repeats were performed for all electrospun yarns and controls (size 2-0 PDS and Vicryl sutures).

2.6. Tensile testing

Braided yarns were tested knotless at a crosshead speed of 50 mm/min with a 5 kN load cell until failure using a Zwick tensile testing machine (Zwick Roell Group, USA). A preliminary investigation with Pincer grips (Zwick Roell Group, USA) yielded inconsistent results and yarn pull through the grip clamps [19]. To generate more reproducible data, custom grips were designed based on tensile grips used in the textile industry for yarns and ropes [20]. These grips were

manufactured to slide onto the existing Zwick grips, as shown in Fig. 4a. Yarn samples were cut into 20 cm sections for testing. Force at break (N), ultimate stress (MPa), guide-to-guide breaking strain (%), and Young's modulus (MPa) were recorded. The cross-sectional area calculations for stress measurements were obtained by multiplying the µCT solid cross-sectional area by (1- overall porosity obtained from Hg porosimetry). Size 2-0 PDS and Vicryl sutures were used as controls. Five experimental repeats were performed for all electrospun yarns and controls.

2.7. Suture pull through

A pull through test was performed using a ballistics gel to mimic a uniform soft tissue surrogate [21,22]. The gel was prepared by dissolving 80 ml gelatine (Knox Unflavored Gelatine, Kraft Foods, Northfield, IL, USA) in 350 ml of boiling water and pouring the mixture into a square mould (23.5 cm × 23.5 cm × 4 cm). The mould was left in a 4 °C fridge for 24 h to solidify. The resulting gel was cut into rectangles (4 cm × 3 cm × 1.2 cm). Yarns were cut into 15 cm pieces and soaked in PBS (Sigma-Aldrich, USA) for 5 min prior to testing. A suture needle (Sterilseal SN1326, Aspen Medical, UK) was attached to the electrospun yarns and used to pass the yarn through the whole gel at 1 cm from the edge of the gel. A Zwick tensile testing machine with a 5 kN load cell (Zwick Roell Group, USA) was used to test each sample. The gel was placed into a small mould and mounted in to lower stationary grip of the machine. The yarn was left untied and clamped to the upper grip. Two different pull through tests were performed to mimic different physiological loading conditions [21–23]. First, the upper grip moved at a rate of 2 mm/min until the yarn pulled through the material. For the second test, the upper grip moved at a rate of 500 mm/min to mimic an abrupt force [21,22]. All braided electrospun yarns, as well as the controls (size 2-0 PDS and Vicryl) were used for each pull through test (n = 5) and the maximum force at pull out (N), strain at pull through (%), and work done until failure (Nmm) was recorded.

2.8. Statistical analysis

For all quantitative analyses, data are presented as mean ± standard deviation. For statistical comparison, a one-way ANOVA followed by a Tukey post-hoc test was performed to identify significance between each group. Graphpad PRISM version 7 software (GraphPad Software Inc., La Jolla, CA, USA) was used for all statistical analysis. Statistical significance was determined at $p < 0.05$, $p < 0.01$, $p < 0.001$, and $p < 0.0001$. Uppercase and lowercase letters represent statistics in figures; an uppercase letter (eg, A) designates that material as significantly greater than every other material with the corresponding lowercase letter (eg, a).

3. Results

3.1. Braiding parameters and braid characteristics

Around 1000 meters of electrospun filament was fabricated at a production speed of 5 meters of stretched filament per hour (0.08 meters per minute) and with a linear density of 9 tex. The braiding process is shown in Fig. 1. Braided yarns were manufactured with continuous electrospun filaments using the Variation Braiding Machine shown in Fig. 1A and B. The filaments were under substantial tension as they passed through yarn carriers and any sections that were not fully hand stretched were drawn out at that point. The production speed for industrial braiding was about 1–3 meters per minute depending on machine input parameters. Based on pilot hand-braiding data from our lab, the use of this machine represents an increase in production speed of about 500%. The various arrangements of carriers used and optical microscope pictures of the final yarn morphology are shown in Fig. 1C. It can be noted that the 8 carrier arrangement forms a closed square

whereas the 20 or 24 carrier arrangements form an open structure with a hollow centre. Table 1 shows the braiding machine parameters, braid size, and braid angle for all yarn configurations. The four braid configurations yielded yarns with diameters between 0.5 and 1 mm. The lower limit of 0.5 mm was chosen to create a tight yarn with a high porosity and the upper limit of 1 mm was chosen to retain good yarn usability. The 8 carrier braid was fabricated with two filaments per carrier as it was projected that one filament per carrier would not yield a braid strong enough to be used as a suture. Braiding with 8 carriers and 2 filaments/carrier produced a yarn with a diameter of 0.5 (± 0.1) mm, which corresponds to USP size 0, whereas braiding with 24 carriers and 1 filament/carrier produced a yarn with a diameter of 1.0 mm (± 0.1), which corresponds to USP size 6. Braiding with 8,12, 20, and 24 carriers resulted in yarns with braid angles of 52°(± 2), 68°(± 2), 70°(± 2), and 74°(± 1).

3.2. Porosity

Fig. 2 shows µCT cross-sectional and longitudinal scans, as well as SEM images of the braided yarns. As anticipated, the 8 carrier configuration resulted in a tight square structure, whereas the 12, 20, and 24 carrier arrangements resulted more flat structures. The hollow centre of the yarn can be seen in the µCT images of the 20 and 24 carrier braids (Fig. 2h and k, respectively). Braid characteristics obtained from µCT scans and Hg porosimetry results are given in Table 2. The overall porosity measured from µCT cross sections was 56% (± 0), 50% (± 2), 60% (± 0), and 66% (± 2) for yarns braided with 12, 8, 20, and 24 carriers, respectively. The smallest yarn cross-sectional area (CSA) of 0.3 (± 0.1) mm² was obtained from the 12 filament braid, whereas the largest CSA of 1.0 (± 0.1) mm² was obtained from the 24 filament braid. Overall porosity measured from Hg porosimetry was 67%, 60%, 65%, and 76% for yarns braided with 12, 8, 20, and 24 carriers, respectively. These porosity results were notably higher than the measurements obtained from the µCT scans. The Hg porosity measurements for control sutures was 28% for the braided Vicryl and 0% for the monofilament PDS. A representative comparison of the pore size distribution from the 20 filament electrospun braid, as well as the PDS and Vicryl sutures, is shown in Fig. 3. The electrospun yarn intrusion curve showed two broad peaks, where the Vicryl curve showed minimal intrusion, and the PDS curve displayed no intrusion. A representative intrusion curve from each of the four electrospun yarns is given as Supplementary Fig. 2.

3.3. Mechanical analysis

3.3.1. Tensile properties

The custom grips used for tensile testing are shown in Fig. 4A and a representative stress-strain graph is shown in Fig. 4B with an emphasis on the toe region in Fig. 4C. Uniaxial tensile testing of the braided yarns until failure was used to calculate the force at break (N), ultimate stress (MPa), breaking strain (%), as well as Young's modulus (MPa), as shown in Fig. 5. All sutures failed in the mid-substance region and showed characteristic toe, linear, and yield regions. The nonlinear mechanical behaviour of the toe region, at 0%–3% of the strain, shown in Fig. 4C, was due to the reorganisation of filaments during early stages of loading. The linear region formed at around 3% of strain, at which point most fibres were engaged. The materials yielded from 12% strain with classic post yield softening. In comparing the different braiding configurations, the average force at break was significantly different between all braids, and higher for braids made with 20 filaments (21 ± 1N) and 24 filaments (25 ± 1N), compared with 16 filaments (15 ± 1N) and 12 filaments (13 ± 1N), as shown in Fig. 5A. The ultimate stress was significantly higher for the 12 filament braid (190.2 ± 31.7 MPa), compared with that of the 16 filament (128.1 ± 16.6 MPa), 20 filament (132.2 ± 10.8 MPa), and 24 filament braids (113.8 ± 8.8 MPa), as shown in Fig. 5c. The Young's

Fig. 1. Assembling multifilament electrospun yarns with an industrial braiding machine. (A) Variation Braiding Machine used to fabricate braided yarns. (B) Electrospun filaments being braided into a continuous yarn. (C) The various carrier arrangements used for manufacturing are shown above, and optical microscope pictures of the final yarns are shown below. Scale bars are 500 μm. It can be noted that the 8 and 12 carrier arrangement form a closed structure, whereas the 20 and 24 carrier arrangement form an open structure with a hollow centre.

Table 1
Braiding parameters and braid characteristics.

Number of carriers	Number of filaments	Number of filaments/ carrier	Braid size (mm)	Braid size (USP)	Braid angle (°)
12	12	1	0.6 (± 0.1)	1	68 (± 2)
8	16	2	0.5 (± 0.1)	0	52 (± 2)
20	20	1	0.8 (± 0.1)	4	70 (± 2)
24	24	1	1.0 (± 0.1)	6	74 (± 1)

Modulus was significantly higher for the 12 filament braid (747.2 ± 7.9 MPa), compared with that of the 16 filament (474.8 ± 24.7 MPa, $p < 0.0001$) and 24 filament braids (489.5 ± 38.1 MPa, $p < 0.0001$), as shown in Fig. 5d.

Significant differences in mechanical properties and behavior were observed in comparing electrospun braided yarns to control sutures. The force to failure was 75 ± 0.3N for Vicryl and 46 ± 0.6N for PDS, which was higher than all of the electrospun yarns ($p < 0.0001$) and

statistically different between each other ($p < 0.0001$). The average ultimate stress was 785 ± 2 MPa and 480 ± 4 MPa for Vicryl and PDS respectively, which was higher than all of the electrospun braid configurations, $p < 0.0001$. The breaking strain was 37 ± 2% for PDS, which was statistically lower than the 20 filament (43.4 ± 1.5%, $p < 0.001$) and 24 filament braids (42.1 ± 1.5%, $p < 0.01$). The breaking strain was 22 ± 3% for Vicryl which was statistically lower than all of the electrospun yarns, $p < 0.0001$. The Young's Modulus was 3959 ± 290 MPa for Vicryl and 1750 ± 64 MPa for PDS, which was statistically higher than all of the electrospun yarns ($p < 0.0001$) and 2–5 times greater than the Young's Modulus of the stiffest electrospun yarn.

3.3.2. Pull through

A custom testing setup was used to perform two pull through tests using a ballistics gel to mimic a uniform soft tissue surrogate, as shown in Fig. 6a [21,22]. Representative gels after 2 mm/min pull through are presented in Fig. 6b, and graphs of the force required to pull through
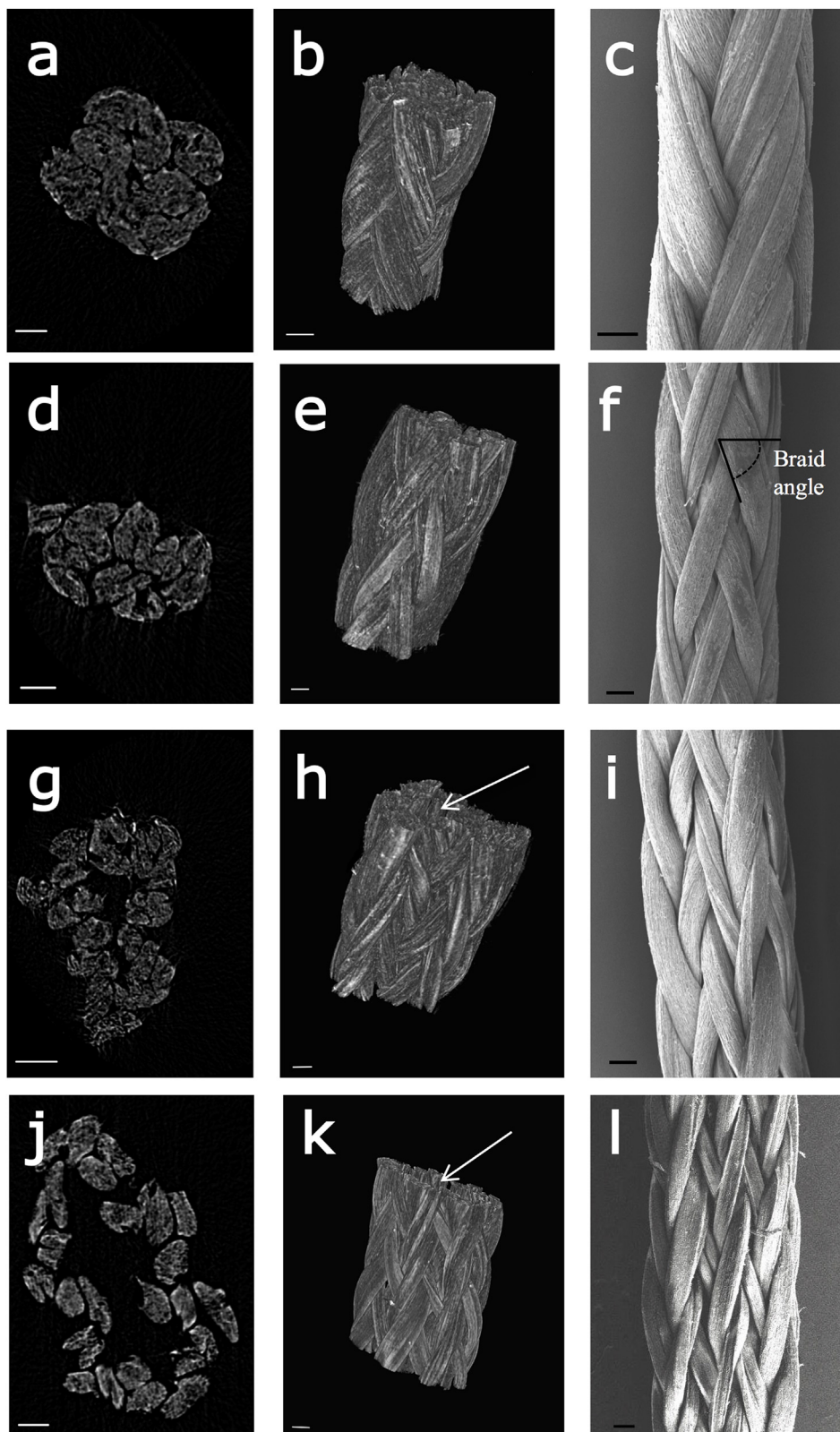
Fig. 2. Microcomputed tomography (μCT) scans and scanning electron microscope images (SEM) of braided electrospun yarns. A cross-sectional scan taken by μCT is shown in (A), (D), (G), and (J), for the 8, 12, 20, and 24 carrier braids, respectively. A longitudinal scan taken by μCT is shown in (B), (E), (H), and (K) for the 8, 12, 20, and 24 carrier braids, respectively. The hollow centre of the yarn can be seen in the images of the 20 and 24 carrier braids, (H) and (K), respectively (white arrows). SEM images were taken to determine yarn morphology and used to measure braid angle, as shown in (C), (F), (I), and (L), for the 8, 12, 20, and 24 carrier braids, respectively. Scale bars are 100 μm for μCT scans and 200 μm for SEM images.

both electrospun yarn and commercial sutures through the ballistics gel at both speeds are shown in Fig. 6c and d. It can be seen that the yarns displayed a different mode of failure when pulled through at 2 mm/min. The monofilament PDS and braided Vicryl pulled a line straight through the gel, whereas the electrospun yarns took out a large section of the gel as it pulled through. Moreover, under both pull through loading conditions, the electrospun sutures displayed a larger force-displacement curve compared with Vicryl and PDS controls. In all cases, there was no failure of the yarn and failure occurred by pull through of the gel.

The mechanical pull through results are shown in Fig. 7. For yarns pulled through at 2 mm/min, the force to failure was significantly

Table 2
μCT and Hg porosimetry data.

Number of carriers (nr of filaments)	μCT		Hg porosimetry		
	Porosity (%)	CSA (mm^2)	Porosity (%)	Intrusion volume (mL/g)	Bulk density at 0.51 psia (g/mL)
12 (12)	56 (± 0)	0.3 (± 0.1)	67 (± 3)	1.0 (± 0)	0.6 (± 0)
8 (16)	50 (± 2)	0.4 (± 0.1)	60 (± 1)	1.0 (± 0)	0.7 (± 1)
20 (20)	60 (± 0)	0.7 (± 0.1)	65 (± 3)	1.4 (± 1)	0.4 (± 0)
24 (24)	66 (± 2)	1.0 (± 0.1)	76 (± 2)	2.0 (± 1)	0.4 (± 0)

higher for the 16 filament braid (2.1 ± 0.2N), compared with the 12 filament (2.1 ± 0.2N, p = 0.0005), 20 filament (2.5 ± 0.4N, p = 0.009) and 24 filament braids (1.9 ± 0.2N, p = 0.012), as well as the PDS (2.3 ± 0.2N, p < 0.0001) and Vicryl sutures (1.8 ± 0.6N, p = 0.002). The percentage strain at the failure force was significantly lower for the 12 filament braid (10.9 ± 0.3%), compared to the 16 filament (14.8 ± 2.4%, p = 0.004), 20 filament (14.9 ± 3.2%, p = 0.02), and 24 filament braids (13.1 ± 2.0%, p = 0.03). For sutures pulled through the gel at 500 mm/min, the force at pull through was significantly lower for the 12 filament braid (0.5 ± 0.1N), compared with the 16 filament (1.0 ± 0.2N, p = 0.02), 20 filament (0.7 ± 0.0N, p = 0.001) and 24 filament braids (0.7 ± 0.1N, p = 0.04), as well as the PDS sutures (0.3 ± 0.0N, p = 0.006). The strain at failure was not significantly different between the braided electrospun yarns or the control sutures. The average work done to pull through was significantly lower for the 12 filament braid (2.1 ± 0.1Nmm) compared to the PDS suture (1.2 ± 0.1Nmm, p = 0.03).

4. Discussion

Previous work has shown that multifilament electrospun yarns have potential for facilitating soft tissue repair [9,24,25], however developments have been limited to hand-braided yarns. Hand braiding restricts the control over yarn properties and the potential translation of these materials to clinical applictions [1,5,6,8,9,12]. Shifting production to an industrial braiding machine that can support continuous electrospun filaments represents the next step in manufacturing braided electrospun yarns suitable for medical use. The aims of this study were to investigate the feasibility in using an industrial braiding machine

with electrospun filaments and to manufacture yarns with various properties. By adjusting the carrier arrangement and filament number, we manufactured and characterized four multifilament yarn designs with various structural and mechanical properties. In support of our hypothesis, we were able to control the properties and increase the rate of production of multifilament yarns. We also found that electrospun yarns were significantly more porous, had a lower tensile strength, and different pull through behavior compared with commercial sutures.

A popular tissue engineering design hypothesis is that a regenerative device should balance mechanical strength with porosity to allow for tissue infiltration, providing a sequential transition in which the regenerated tissue assumes function as the material degrades [26]. Developing such a device would require collaborative efforts between experts from different disciplines to develop a bioactive suture that can mechanically approximate tissue, facilitate ingrowth of tissue, have a suitable degradation rate to be replaced by newly formed tissue, and have favorable handling properties [27,28]. Numerous studies have indicated that many as-spun electrospun materials have neither the required mechanical or handling properties for use in clinical applications nor the appropriate pore dimensions for cellular infiltration [29–31]. Our group has previously developed a fabrication method to collect continuous electrospun filaments [13], opening the possibility of using industrial braiding technology to manufacture more robust and complex yarns. Some previous work used mini-type braiding machines with electrospun material, however these machines were restricted to a fixed number of carriers [4,7,24]. Although the upscale of electrospun filaments is still a limiting factor in the production of multifilament yarns, the fact that an industrial machine could be used to braid filaments in the current study is also an indirect demonstration of the sufficiently scaled up filament production. The versatility of the Variation Braiding Machine used in the current study is useful for designing yarns that accommodate for a range of mechanical and structural properties displayed by soft tissues. A better understanding of the effect of industrial braiding on the modulation of yarn properties is necessary to design implants that are tissue specific as well as to manufacture reproducible yarns that meet quality control standards for clinical trials. We found it fairly straightforward to use electrospun polydioxanone filaments with the braiding carrier springs, once the tension in the carriers was optimised. By varying the filament number and carrier arrangement, we fabricated four yarns that fit our design criteria of a diameter of 0.5–1 mm. Our results showed that the tight and narrow 8 and 12 carrier yarns had smaller braid angles whereas the looser and more hollow 20 and 24 carrier yarns had larger braid angles.
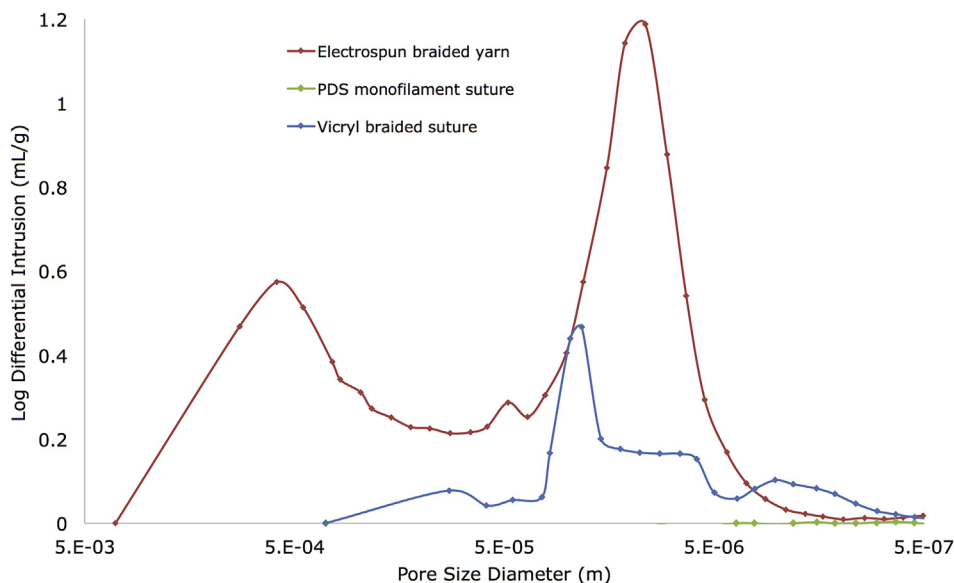

Fig. 3. Pore size distribution in braided electrospun yarns measured by Hg porosimetry. A representative comparison between an electrospun braided yarn with 20 filaments (0.8 ± 0.1 mm), PDS monofilament suture (USP size 2-0, 0.5 mm), and Vicryl braided suture (USP size 2-0, 0.5 mm) is shown. The electrospun yarn intrusion curve showed two broad peaks, where the Vicryl curve showed minimal intrusion, and the PDS curve showed no intrusion.
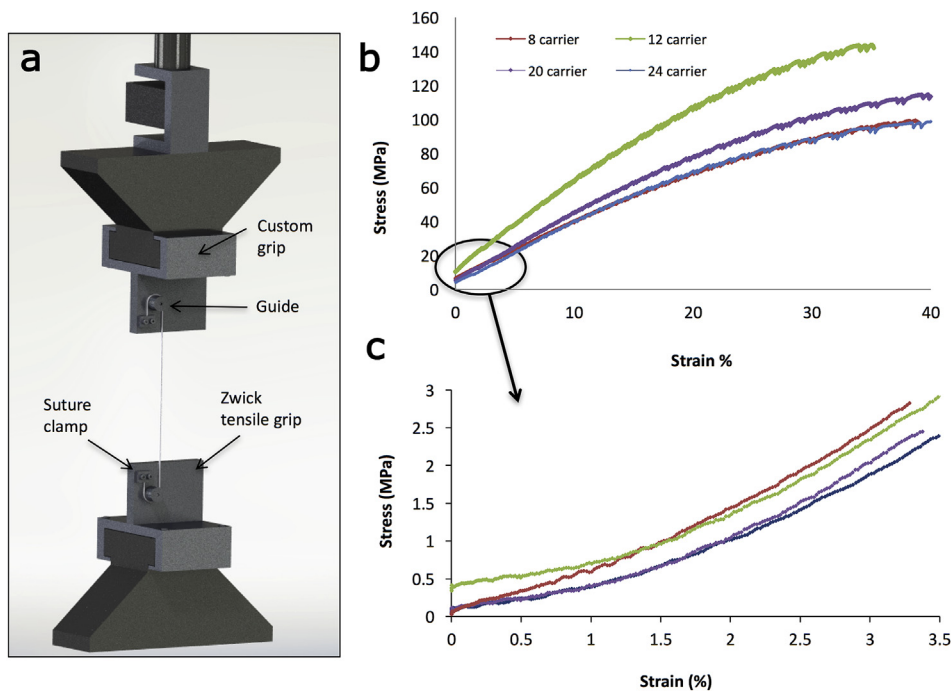
Fig. 4. Tensile testing of braided electrospun yarns. (A) Custom grips used for tensile testing improve yarn grip and slide onto existing Zwick Pincer grips. (B) Representative stress-strain graphs of 8,12,20, and 24 carrier yarns showing characteristic toe, linear, and yield regions. (C) Emphasis on the toe region at 0–3.5% of strain shows nonlinear mechanical behavior due to reorganization of filaments during early stages of loading.

The relationship between braid angle and tightness of braid has been noted before [9]. Czaplewski et al. hand-braided multifilament yarns with the same number of filaments but with varying braid angles, or stiches per inch (SPI) – a unit to measure one filament crossing over another [9]. The authors found that looser braids with larger braid angles were more porous and better supported the expression of tendon and ligament associated markers and induced elongated cell morphology similar to tendon and ligament fibroblasts [9]. Notably, the
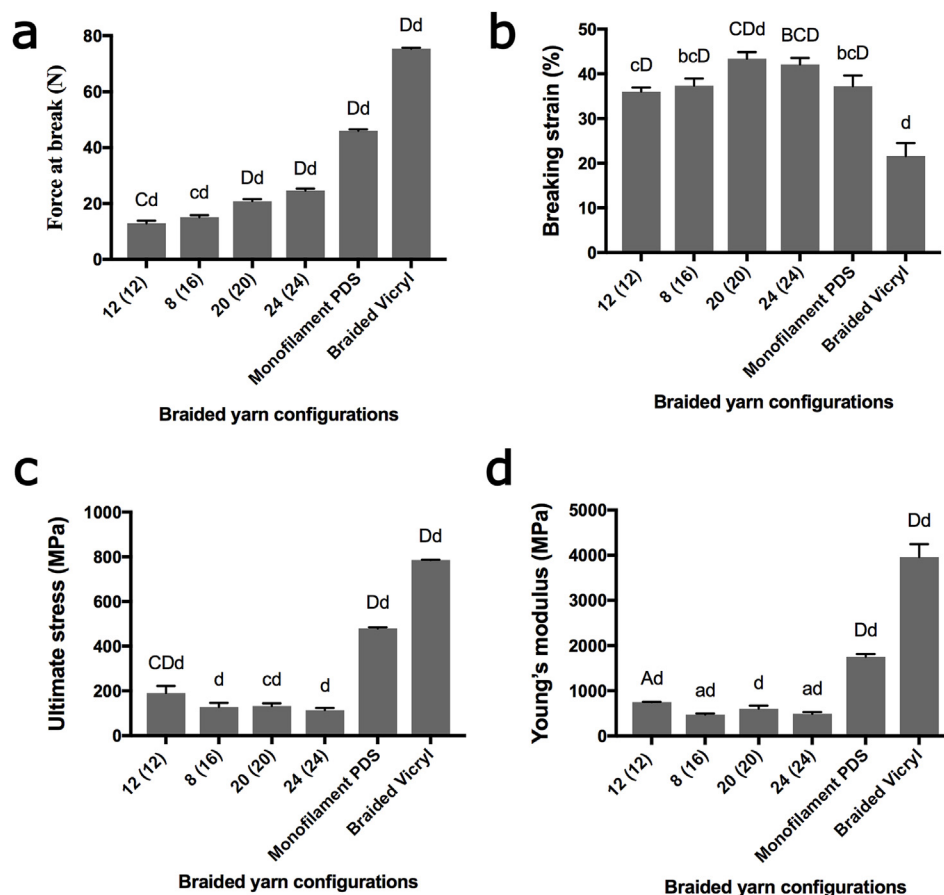

Fig. 5. Tensile properties of braided electrospun yarns. (A) Force at break (N), (B) Breaking strain (%), (C) Ultimate stress (MPa), (D) Young's modulus (MPa). Statistical significance was determined at Aa < 0.05, Bb < 0.01, Cc < 0.001, Dd < 0.0001.
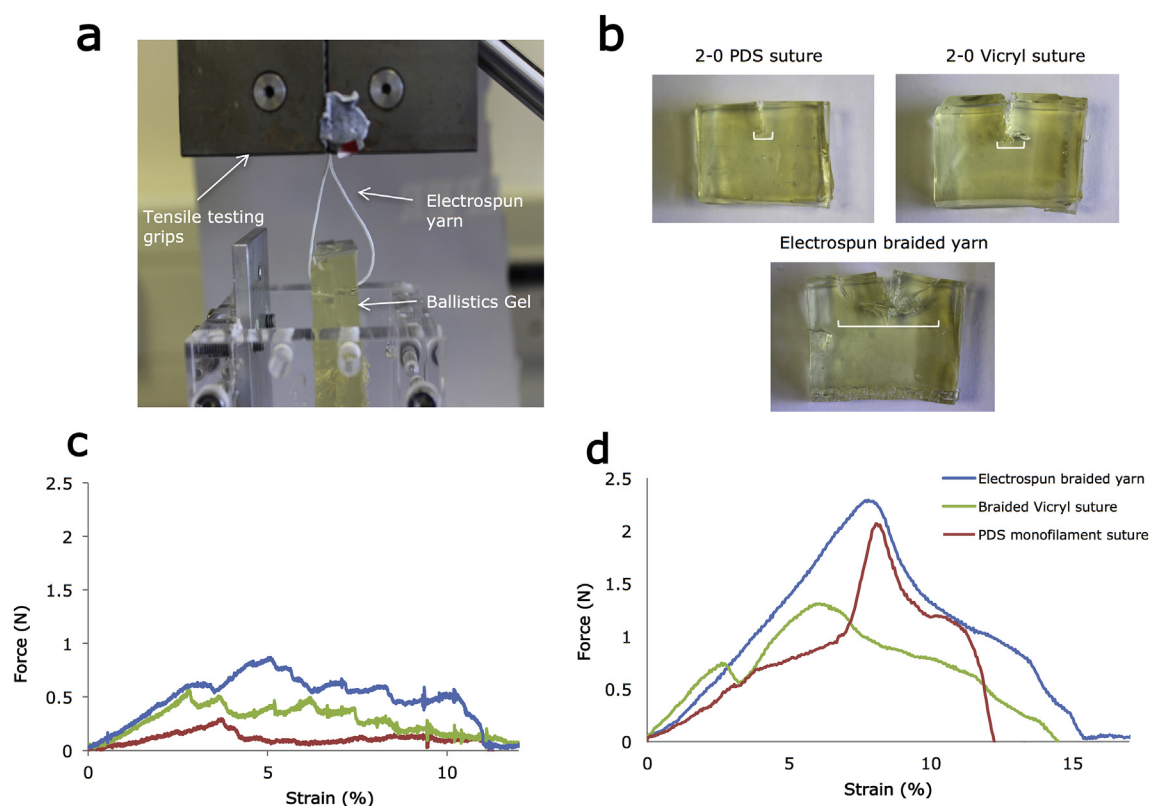
Fig. 6. Pull through testing of braided electrospun yarns. (A) Custom testing setup used for yarn pull through a ballistics gel. (B) Ballistic gel after pull through at 2 mm/min of 2-0 PDS (top left), 2-0 Vicryl (top right), and electrospun braided yarn (bottom), resulting in a different fracture profile of the gel between the yarns tested. White brackets show surface area of gel that was pulled through. (C) Representative graph of the force required to pull through the ballistics gel at 2 mm/min, for an electrospun yarn as well as PDS and Vicryl suture controls. (D) Representative graph of the force required to pull through the ballistics gel at 500 mm/min, for an electrospun yarn as well as PDS and Vicryl suture controls.

braid angle range explored by Czaplewski et al. (47°–67°) was slightly more narrow than the range of our braiding angles (52°–74°), however the direct relationship between braid angle and porosity was also observed within the parameter space tested here. Moreover, our results show that using an industrial machine for braiding substantially improved the repeatability of the yarn properties compared to previous studies using hand-braided yarns. The standard deviation of moduli for our braided yarns ranged between 1% and 11%. In comparison, hand-braided electrospun yarns in previous studies report standard deviations of moduli ranging between 15% and 86% [1,8]. This reduction in variability between yarn samples has implications for both fundamental studies investigating the relationship between yarn properties and cellular behavior, as well as for facilitating the translation of these yarns for clinical use.

Yarn porosity is an important design factor modulating cellular response, mechanical properties, and degradation [32–34]. The rationale for investigating yarn porosity in the current study was to compare μCT scanning and Hg porosimetry methods, as well as to compare the porosity between electrospun braided yarns and commercial sutures. Both μCT [35] and Hg porosimetry [34] are established methods for measuring the porosity of electrospun materials, however our results showed that μCT underestimated overall porosity by around 10% compared with Hg porosimetry. While μCT can be useful for a gross calculation of pore size, the μCT used in the current study was limited to measuring pore sizes greater than 0.9 μm, rendering it unsuitable for measuring the porosity of filaments made up of micro- or nanoscale pores. In contrast, the Hg porosimeter had a resolution of 0.005 μm and revealed that electrospun yarns were more porous and showed a range of pore sizes compared with commercial sutures. The electrospun yarn intrusion curve showed two main peaks, reminiscent of two pore sizes: small pores in between submicron fibres and larger pores measured

both in the open spaces between filaments and in the hollow core for the 20 and 24 filament braids. The initial broad peak was likely due to interstitial filling when most of the open spaces between the filaments are filled by mercury. The second more narrow main peak is genuine intrusion of filling in between the fibres. The braided Vicryl intrusion graph shows some interstitial filling and no genuine intrusion, indicating minimal space between the braided bundles of fibres. As anticipated, the monofilament PDS intrusion graph showed no intrusion. In the context of fibres for medical use, the microporous architecture of electrospun material is crucial for cell attachment and nutrient transport. Previous work has focused on twisted monofilaments [35–37] made from sheets of densely aligned fibres, however many studies found a lack of cellular infiltration into the yarn, which could have detrimental consequences to the long-term success of the implant [1,35]. Bosworth et al. found that most cells remained on the outer periphery of their twisted monofilament polycaprolactone yarn, with minimal infiltration [35]. The authors noted that the approximate diameter of hMSCs is 20 μm, which is considerably larger than the spaces between their twisted aligned nanofibres. A hierarchical yarn architecture, as developed in the current study, with dense filaments braided into multifilament yarns with larger meso- or macroscopic pores is postulated to improve cellular infiltration of cells too big to fit in micropores between fibres [38]. The presence of a hollow core, such as in the 20 and 24 filament braids, will be particularly interesting to investigate with regard to driving cellular infiltration. Hg porosimetry revealed that the main pore sizes for the 20 and 24 filament yarns were on the order of 10–100 times larger than those of the 12 and 16 filament yarns and larger than the average diameter of hMSCs (as seen in the Supplementary Figure). These differences were confirmed with μCT, which show both a large core in the centre of the 20 and 24 filament yarns, as well as larger spaces between the filaments. It is possible that
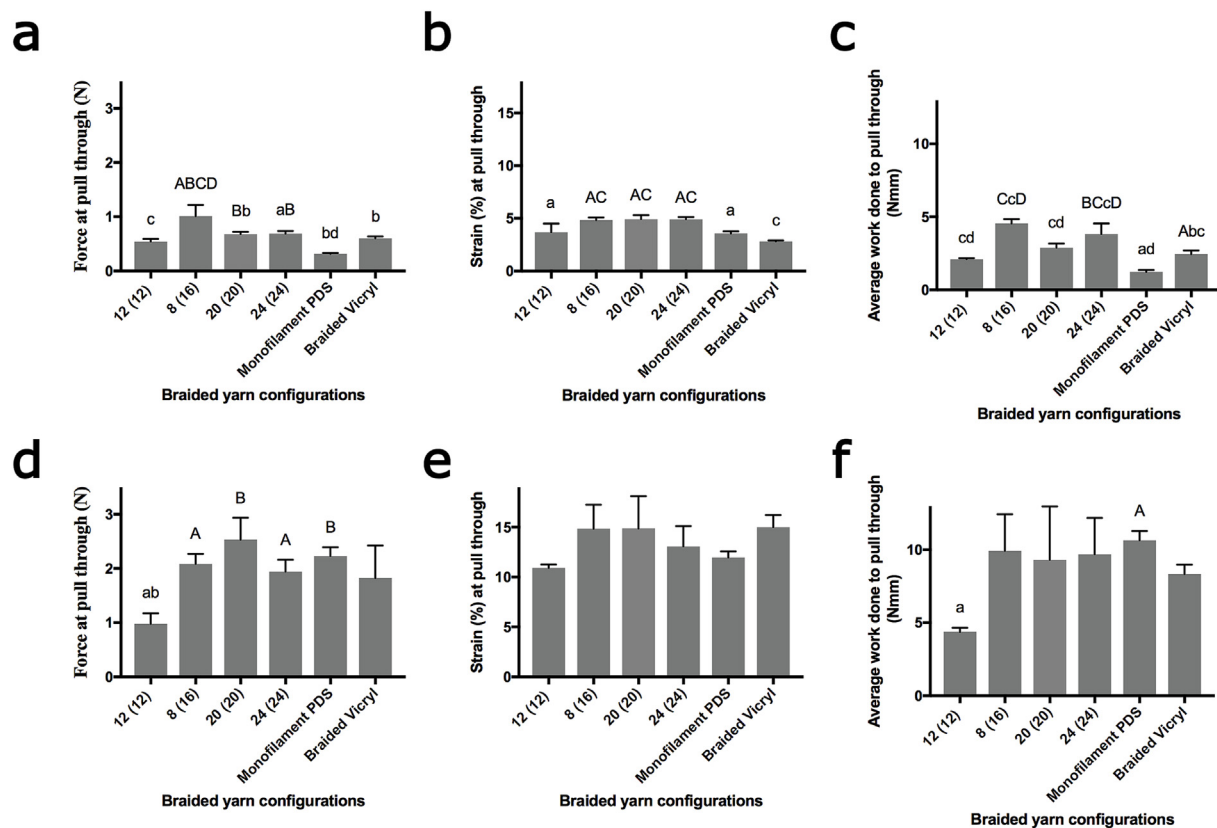
Fig. 7. Pull through properties of braided electrospun yarns. (A–C) Pull through of all electrospun braided configurations and control sutures pulled through at 2 mm/min. (A) Force at pull through (N), (B) Strain at pull through (%), (C) Average work done to pull through (Nmm). (D–F) Pull through of all electrospun braided configurations and control sutures pulled through at 500 mm/min. (D) Force at pull through (N), (E) Strain at pull through (%), (F) Average work done to pull through (Nmm). Statistical significance was determined at Aa < 0.05, Bb < 0.01, Cc < 0.001, Dd < 0.0001.

the hollow core could close upon dynamic loading, however this effect can be minimised with the introduction of axial or inlay yarns. Future work will use Hg porosimetry and BET surface area analysis methods to explore the influence of yarn pore sizes and surface area on cellular attachment and infiltration.

Our mechanical testing results revealed that the mechanical behavior differed between electrospun yarns and that the length and size of the toe, linear, and yield regions depended on the number of filaments. Smaller braids with 12 and 16 filaments displayed a longer toe region, whereas the larger, looser braids with 20 and 24 filaments, displayed the longest yield regions and lowest stiffness. This difference in mechanical behaviour is likely attributed to differences in filament arrangement affecting fibre repositioning during mechanical loading, which is consistent with findings from other work [6,8,9]. However the implications these differences have on yarn viability would have to be assessed with a dynamic bioreactor system or an *in vivo* study.

Tensile testing results revealed that none of the electrospun yarns closely matched the mechanical properties of commercially used PDS and Vicryl sutures. PDS is made from polydioxanone extruded as a single monofilament, whereas Vicryl is a copolymer of polyglycolide-L-lactide, which is extruded as a bundle of fibres and braided into a multifilament yarn [28]. Unlike electrospinning, there is no dilution of the polymer for fabrication, explaining the vastly different force at break and ultimate stress measured between the sutures and electrospun yarns. There were also differences in mechanical properties observed between electrospun yarns. While no previous work has explored electrospun multifilament polydioxanone yarns to serve as a comparison, numerous studies have investigated the mechanical properties of yarns with different filament numbers [6,8,9]. In contrast to the current study, Czapleski et al. found that looser braids showed the highest modulus and strength [9]. In the current study, the opposite

trend was observed: looser braids with larger braid angles displayed increased strain and decreased modulus and stress. Such a discrepancy could be explained by the fact that changing the filament number in the current study outweighed the potential mechanical difference due to filament organisation observed by Czaplewski et al. Barber et al. fabricated yarns made of 3, 4, or 5 filaments and observed variable stiffnesses within the initial 10% of deformation, on a similar scale to the differences observed in the current study [6]. The stiffnesses observed in the current study and by Barber et al. fell within the range of cyclic uniaxial tension commonly used for *in vitro* culture of tendon and ligament tissue engineering scaffolds [39,40]. In the context of multifilament yarns for medical use, our versatile fabrication method could be useful in future work to produce yarns that accommodate for the range of stiffnesses and mechanical strengths displayed by soft tissues *in vivo*.

Our pull through testing revealed that electrospun yarns possessed different pull through properties compared with existing commercial suture materials. Few studies on engineered patches or yarns measure pull through strength, despite its established importance for clinical implementation [22]. Electrospun yarns possessed a higher force at pull through, work done to failure, and a different mode to failure, compared to PDS and Vicryl sutures. Similar results were observed by Duminian et al., who measured the pull through strength of a novel highly porous mesh suture [21]. Compared to a commercial suture composed of the same material, they found that the mesh suture required a doubling of force to pull through a ballistics gel, attributing the difference to the increased surface area and diameter of the mesh suture [21]. The differences observed between commercial sutures and electrospun yarns in the current study can be attributed to the higher surface area of electrospun materials, increasing the size of the suture-gel interface and lowering the force measured at any one point. This increase spread in

load area manifested in a very different fracture profile of the gel for the slower 2 mm/min pull through experiments. The increased surface area of the pulled through gel is directly related to the energy of the system, suggesting that the structural configuration of electrospun material allowed for more dissipation of energy at low pull through rates [41]. As with any material at higher rates, the faster 500 mm/min pull through experiments resulted in minimal energy dissipation.

There are several limitations to be considered. First, electrospun yarns were all made with different filament numbers, making it difficult to discern mechanical differences due to filament arrangement alone. However, the aim of this feasibility study was to show the possibility of braiding electrospun yarns with different filament numbers and carrier arrangements. This has not been previously done and has important implications for optimizing functional tissue engineering yarns. Second, we only collected porosity data from two runs with the Hg porosimeter. As such, the porosity comparison between electrospun yarns is given in the Appendix and should be taken as indicative only. Future work will explore the relationship between yarn porosity and cell behaviour in more depth. Our study also presents several unique strengths. This is the first study to investigate the macroscale architecture of multi-filament electrospun yarns, which is a necessary step to optimise functional materials for medical use. It is also the first study to explore the use of an industrial braiding machine with electrospun filaments. Moreover, while previous studies have assessed some structural aspects of braided electrospun yarns, no study has compared the properties of electrospun yarns directly to those of commercial sutures.

5. Conclusion

This study explored using an industrial braiding machine to upscale and control the production of electrospun yarns intended for medical use. We demonstrated that using an industrial braiding machine was possible with electrospun filaments and we produced yarn designs with different porosities, mechanical strengths and suture pull through characteristics. Compared to commercial sutures, electrospun braided yarns were more porous, had a lower tensile strength, and resulted in different pull through behavior, suggesting that electrospun yarns allowed for more dissipation of energy at low pull through rates. Future work will investigate the biological response to the different yarn designs. Integrating electrospun filaments into existing industrial braiding production lines to manufacture multifilament yarns is important for both fundamental studies on yarn properties and to ease the translation of multifilament yarns beyond preclinical trials.

Acknowledgements

Appendix A. Supplementary data

Supplementary Figure: Pore size distribution between different electrospun yarn designs measured by Hg porosimetry. A representative comparison between electrospun braided yarns made up of 12, 16, 20, and 24 filaments, is shown. The 20 and 24 filament braids show main peaks on the order of 10–100 times larger than those of the 12 and 16 filament braids.

Supplementary data related to this article can be found at http://dx.doi.org/10.1016/j.polymertesting.2018.05.014.

Appendix

Table A1
Mechanical properties of braided electrospun yarns and commercial sutures (n = 5).

Nr of braiding carriers (nr of filaments)	Force at break (N)	Breaking strain (%)	Ultimate stress (MPa)	Young's modulus (MPa)
12 (12)	12.9 ± 0.9	36.0 ± 0.9	190.2 ± 31.7	747.2 ± 7.9
8 (16)	15.1 ± 0.8	37.3 ± 1.6	128.1 ± 16.6	474.8 ± 24.7
20 (20)	20.9 ± 0.7	43.4 ± 1.5	132.2 ± 10.8	603.0 ± 67.9
24 (24)	24.7 ± 0.7	42.1 ± 1.5	113.8 ± 8.8	489.5 ± 38.1
Monofilament PDS 2-0	46.0 ± 0.6	37.2 ± 2.4	479.8 ± 4.5	1750.3 ± 64.5
Braided Vicryl 2–0	75.4 ± 0.3	21.6 ± 2.9	785.4 ± 1.5	3959.0 ± 289.5

Table A2
Braided electrospun yarns and commercial sutures pull through ballistics gel at 2 mm/min (n = 3).

Nr of braiding carriers (nr of filaments)	Force at pull through (N)	Strain (%) at pull through	Average work done to pull through (Nmm)
12 (12)	0.5 ± 0.1	3.7 ± 0.8	2.1 ± 0.1
8 (16)	1.0 ± 0.2	4.8 ± 0.2	4.6 ± 0.3
20 (20)	0.7 ± 0.0	4.9 ± 3.8	2.9 ± 0.3
24 (24)	0.7 ± 0.1	4.9 ± 0.2	3.8 ± 0.7
Monofilament PDS 2-0	0.3 ± 0.0	3.6 ± 0.2	1.2 ± 0.1
Braided Vicryl 2-0	0.6 ± 0.1	2.8 ± 0.1	2.4 ± 0.3

Table A3
Braided electrospun yarns and commercial sutures pull through ballistics gel at 500 mm/min (n = 3).

Nr of braiding carriers (nr of filaments)	Force at pull through (N)	Strain (%) at pull through	Average work done to pull through (Nmm)
12 (12)	1.0 ± 0.2	10.9 ± 0.3	4.4 ± 0.3
8 (16)	2.1 ± 0.2	14.8 ± 2.4	9.9 ± 2.5
20 (20)	2.5 ± 0.4	14.9 ± 3.2	9.3 ± 3.7
24 (24)	1.9 ± 0.2	13.1 ± 2.0	9.7 ± 2.5
Monofilament PDS 2-0	2.3 ± 0.2	12.0 ± 0.6	10.6 ± 0.6
Braided Vicryl 2-0	1.8 ± 0.6	15.0 ± 1.2	8.3 ± 0.6

References

[1] B.B. Rothrauff, B.B. Lauro, G. Yang, R.E. Debski, V. Musahl, R.S. Tuan, Braided and stacked electrospun nanofibrous scaffolds for tendon and ligament tissue engineering, Tissue Eng. 23 (9–10) (2017) 378–389, http://dx.doi.org/10.1089/ten.tea.2016.0319.
[2] D.H. Reneker, A.L. Yarin, Electrospinning jets and polymer nanofibers, Polymer (Guildf) 49 (10) (2008) 2387–2425, http://dx.doi.org/10.1016/j.polymer.2008.02.002.
[3] B. Ma, J. Xie, J. Jiang, F.D. Shuler, D.E. Bartlett, Rational design of nanofiber scaffolds for orthopedic tissue repair and regeneration, Nanomedicine (Lond) 8 (9) (2013) 1459–1481, http://dx.doi.org/10.2217/nnm.13.132.
[4] W. Hu, Z.-M. Huang, X.-Y. Liu, Development of braided drug-loaded nanofiber sutures, Nanotechnology 21 (31) (2010) 315104, , http://dx.doi.org/10.1088/0957-4484/21/31/315104.
[5] U. Ali, Y. Zhou, X. Wang, T. Lin, Direct electrospinning of highly twisted, continuous nanofiber yarns, J. Text. Inst. 103 (1) (2012) 80–88, http://dx.doi.org/10.1080/00405000.2011.552254.
[6] J.G. Barber, A.M. Handorf, T.J. Allee, W.-J. Li, Braided nanofibrous scaffold for tendon and ligament tissue engineering, Tissue Eng. 19 (11–12) (2013) 1265–1274, http://dx.doi.org/10.1089/ten.tea.2010.0538.
[7] W. Hu, Z.-M. Huang, S.-Y. Meng, C. He, Fabrication and characterization of chitosan coated braided PLLA wire using aligned electrospun fibers, J. Mater. Sci. Mater. Med. 20 (11) (2009) 2275–2284, http://dx.doi.org/10.1007/s10856-009-3797-y.
[8] J.W. Freeman, M.D. Woods, C.T. Laurencin, Tissue engineering of the anterior cruciate ligament using a braid–twist scaffold design, J. Biomech. 40 (2007) 2029–2036, http://dx.doi.org/10.1016/j.jbiomech.2006.09.025.
[9] S.K. Czaplewski, T.-L. Tsai, S.E. Duenwald-Kuehl, R. Vanderby, W.-J. Li, Tenogenic differentiation of human induced pluripotent stem cell-derived mesenchymal stem cells dictated by properties of braided submicron fibrous scaffolds, Biomaterials 35 (25) (2014) 6907–6917, http://dx.doi.org/10.1016/j.biomaterials.2014.05.006.
[10] S. Wu, B. Duan, P. Liu, C. Zhang, X. Qin, J.T. Butcher, Fabrication of aligned nanofiber polymer yarn networks for anisotropic soft tissue scaffolds, ACS Appl. Mater. Interfaces 8 (26) (2016) 16950–16960, http://dx.doi.org/10.1021/acsami.6b05199.
[11] R. Abhari, C. AJ, P. Mouthuy, Multifilament electrospun scaffolds for soft tissue reconstruction, in: V. Guarino, L. Ambrosio (Eds.), Electrofluidodynamic Technologies for Biomaterials and Medical Devices, Elsevier Limited, 2018, pp. 295–328.
[12] S. Wu, B. Duan, P. Liu, C. Zhang, X. Qin, J.T. Butcher, Fabrication of aligned nanofiber polymer yarn networks for anisotropic soft tissue scaffolds, ACS Appl. Mater. Interfaces 8 (26) (2016) 16950–16960, http://dx.doi.org/10.1021/acsami.6b05199.
[13] P.-A. Mouthuy, N. Zargar, O. Hakimi, E. Lostis, A. Carr, Fabrication of continuous electrospun filaments with potential for use as medical fibres, Biofabrication 7 (2) (2015) 25006 http://stacks.iop.org/1758-5090/7/i=2/a=025006.
[14] R.E. Abhari, P.-A. Mouthuy, N. Zargar, C. Brown, A. Carr, Effect of annealing on the mechanical properties and the degradation of electrospun polydioxanone filaments, J. Mech. Behav. Biomed .Mater 67 (2017), http://dx.doi.org/10.1016/j.jmbbm.2016.11.023.
[15] Y. Kyosev (Ed.), Advances in Braiding Technology: Specialized Techniques and Applications, Woodhead Publishing Series in Textiles, 2016.
[16] N. Goonoo, R. Jeetah, A. Bhaw-Luximon, D. Jhurry, Polydioxanone-based bio-materials for tissue engineering and drug/gene delivery applications, Eur. J. Pharm. Biopharm. 97 (2015) 371–391, http://dx.doi.org/10.1016/j.ejpb.2015.05.024.
[17] M a Sabino, S. González, L. Márquez, J.L. Feijoo, Study of the hydrolytic degradation of polydioxanone PPDX, Polym. Degrad. Stabil. 69 (2) (2000) 209–216, http://dx.doi.org/10.1016/S0141-3910(00)00062-8.
[18] J. Xie, X. Li, Y. Xia, Putting electrospun nanofibers to work for biomedical research, Macromol. Rapid Commun. 29 (22) (2008) 1775–1792, http://dx.doi.org/10.1002/marc.200800381.
[19] S. Chaudhury, Mechanical and Chemical Properties of Rotator Cuff Tendons, (2012) http://solo.bodleian.ox.ac.uk/primo_library/libweb/action/display.do?tabs=detailsTab&ct=display&fn=search&doc=oxfaleph019632192&indx=1&recIds=oxfaleph019632192&recIdxs=0&elementId=0&renderMode=poppedOut&displayMode=full&frbrVersion=&frbg=&vl(254947567UI0) , Accessed date: 20 May 2017.
[20] ADMET - Rope and Thread. http://www.admet.com/products/test-fixtures-and-accessories/test-fixtures/rope-and-thread/. Accessed July 31, 2017.
[21] Dumanian GA, Tulaimat A, Dumanian ZP. Experimental study of the characteristics of a novel mesh suture. doi:https://doi.org/10.1002/bjs.9853.
[22] M. Staat, E. Trenz, P. Lohmann, et al., New measurements to compare soft tissue anchoring systems in pelvic floor surgery, J. Biomed. Mater. Res. B Appl. Biomater. 100B (4) (2012) 924–933, http://dx.doi.org/10.1002/jbm.b.32654.
[23] A. Subramanian, D. Vu, G.F. Larsen, Hsin-Yi Lin, Preparation and evaluation of the electrospun chitosan/PEO fibers for potential applications in cartilage tissue engineering, J. Biomater. Sci. Polym. Ed. 16 (7) (2012) 861–873.
[24] J.A. Cooper, H.H. Lu, F.K. Ko, J.W. Freeman, C.T. Laurencin, Fiber-based tissue-engineered ligament replacement: design considerations and in vitro evaluation, Biomaterials 26 (13) (2005) 1523–1532, http://dx.doi.org/10.1016/j.biomaterials.2004.05.014.
[25] S. Sahoo, H. Ouyang, J.C.-H. Goh, T.E. Tay, S.L. Toh, Characterization of a novel polymeric scaffold for potential application in tendon/ligament tissue engineering, Tissue Eng. 12 (1) (2006) 91–99, http://dx.doi.org/10.1089/ten.2006.12.ft-8.
[26] S.J. Hollister, Porous scaffold design for tissue engineering, Nat. Mater. 4 (7) (2005) 518–524, http://dx.doi.org/10.1038/nmat1421.
[27] King MW, Gupta BS (Bhupender S., Guidoin R. Biotextiles as Medical Implants.
[28] R. Abhari, J. Martins, H. Morris, M. PA, A. Carr, Synthetic sutures: clinical evaluation and future developments, J. Biomater. Appl. 0 (0) (2017) 1–12, http://dx.doi.org/10.1177/0885328217720641.
[29] N. Bhardwaj, S.C. Kundu, Electrospinning: a fascinating fiber fabrication technique, Biotechnol. Adv. 28 (3) (2010) 325–347, http://dx.doi.org/10.1016/j.biotechadv.2010.01.004.
[30] M.C. Phipps, W.C. Clem, J.M. Grunda, G.A. Clines, S.L. Bellis, Increasing the pore sizes of bone-mimetic electrospun scaffolds comprised of polycaprolactone, collagen I and hydroxyapatite to enhance cell infiltration, Biomaterials 33 (2) (2012) 524–534, http://dx.doi.org/10.1016/j.biomaterials.2011.09.080.
[31] S. Khorshidi, A. Solouk, H. Mirzadeh, et al., A review of key challenges of electrospun scaffolds for tissue-engineering applications, J. Tissue Eng. Regen. Med. 10 (9) (2016) 715–738, http://dx.doi.org/10.1002/term.1978.
[32] M. Akbari, A. Tamayol, S. Bagherifard, et al., Textile Technologies and tissue engineering: a path toward organ weaving, Adv Healthc Mater 5 (2016) 751–766.
[33] K. Vuornos, M. Björninen, E. Talvitie, et al., Human adipose stem cells differentiated on braided polylactide scaffolds is a potential approach for tendon tissue engineering, Tissue Eng. 22 (5–6) (2016) 513–523, http://dx.doi.org/10.1089/ten.tea.2015.0276.
[34] H.H. Lu, J.A. Cooper, S. Manuel, et al., Anterior cruciate ligament regeneration using braided biodegradable scaffolds: in vitro optimization studies, Biomaterials 26 (23) (2005) 4805–4816, http://dx.doi.org/10.1016/j.biomaterials.2004.11.050.
[35] L.A. Bosworth, S.R. Rathbone, R.S. Bradley, S.H. Cartmell, Dynamic loading of electrospun yarns guides mesenchymal stem cells towards a tendon lineage, J. Mech. Behav. Biomed. Mater 39 (2014) 175–183, http://dx.doi.org/10.1016/j.jmbbm.2014.07.009.
[36] J. Wu, C. Huang, W. Liu, et al., Cell infiltration and vascularization in porous nanoyarn scaffolds prepared by dynamic liquid electrospinning, J. Biomed. Nanotechnol. 10 (4) (2014) 603–614, http://dx.doi.org/10.1166/jbn.2014.1733.
[37] L.A. Bosworth, N. Alam, J.K. Wong, S. Downes, Investigation of 2D and 3D electrospun scaffolds intended for tendon repair, J. Mater. Sci. Mater. Med. 24 (6) (2013) 1605–1614, http://dx.doi.org/10.1007/s10856-013-4911-8.
[38] S. Zhong, Y. Zhang, C.T. Lim, Fabrication of large pores in electrospun nanofibrous scaffolds for cellular infiltration: a review, Tissue Eng. B Rev. 18 (2) (2012) 77–87, http://dx.doi.org/10.1089/ten.TEB.2011.0390.
[39] Z. Feng, M. Ishibashi, Y. Nomura, T. Kitajima, T. Nakamura, Constraint stress, microstructural characteristics, and enhanced mechanical properties of a special fibroblast-embedded collagen construct, Artif. Organs 30 (11) (2006) 870–877, http://dx.doi.org/10.1111/j.1525-1594.2006.00314.x.
[40] N. Sawaguchi, T. Majima, T. Funakoshi, et al., Effect of cyclic three-dimensional strain on cell proliferation and collagen synthesis of fibroblast-seeded chitosan-hyaluronan hybrid polymer fiber, J. Orthop. Sci. 15 (4) (2010) 569–577, http://dx.doi.org/10.1007/s00776-010-1488-7.
[41] Griffith AA. The phenomena of rupture and flow in Solids. Philos. Trans. R. Soc. Lond. - Ser. A Contain. Pap. a Math. or Phys. Character. 221:163–198. doi:https://doi.org/10.2307/91192.